Synthesis of alpha-alumina nanoribbons: characterization and their morphological evolution

Guang Shao · Huijuan Yu · Wei Zeng · Hai-Yang Liu

Abstract Single crystalline α-alumina nanoribbons were synthesized by reacting aluminum with silicon monoxide at high temperature. The products were characterized by X-ray diffraction (XRD), scanning electron microscopy (SEM), transmission electron microscope (TEM), and high-resolution transmission electron microscope (HRTEM). The intense peaks of XRD pattern indicate that the prepared nanoribbons have a high degree of crystallinity. In the present work, silicon monoxide was used as an oxidant and precursor, which served to control the reaction rate. An interesting morphological evolution that nanoribbons resulted from nanosaws was described, and these novel nanosaws were also carefully characterized.

Introduction

To date, extensive efforts have been devoted to the fabrication of well-arranged nanomaterials due to their interesting physical properties and potential application in numerous fields [1–3]. And the fabrication of one-dimensional (1D) nanostructures is especially required for their special morphologies and transport properties [4, 5].

Aluminum oxides are widely used materials with various technological advantages such as adsorbents, ceramics, catalyst supports, and bifunctional catalysts in chemical and petrochemical industry [6–8]. Currently, 1D-nanostructured aluminum oxides are of great interest in both academia and industry owing to their interesting characteristics and possible applications. Many efforts have been dedicated to creating 1D-nanostructured alumina and investigating the mechanisms of its formation. Widely employed methods to prepare 1D inorganic materials are physical evaporation [9, 10], laser ablation [11], vapor deposition [12, 13], and solvothermal way [14].

Essentially, most of these methods proceed through a vapor phase growth procedure via either a vapor–liquid–solid (VLS) or a vapor–solid (VS) pathway [15, 16]. Guitian and co-workers [16–18] have prepared α-alumina fiber and ribbon structures by thermal treatment of Al metal with SiO_2 in the presence of Fe_2O_3 as catalyst under a stream of argon at 1300–1500 °C, which occurred via a VLS process. And a modified VLS deposition process could be applied to produce chromium-doped α-alumina whiskers [19]. Crystalline alumina nanowires and nanotrees were obtained at elevated temperatures in a catalyst-assisted process using iron as catalyst, which actually proceeded via a VS route [20].

Moreover, different morphologies of alumina have been fabricated, such as nanowires [21–23], nanofibers [24, 25], nanoribbons [17], nanotubes [26, 27], nanoring [28], and nanotrees [29]. Nanoribbons hold a unique position because of their special morphology in the easy fabrication of nanodevices. Yet, the growth mechanism of nanoribbons is still obscure. In this paper, we have successfully synthesized α-alumina nanoribbons via a high temperature method, and the morphological evolution of nanoribbons originating from nanosaws was observed, which could explain how these α-alumina nanoribbons were formed.

Experimental section

A horizontal alumina tube was mounted inside a high-temperature tube furnace. SiO powder (0.50 g, 99.99%,

G. Shao (✉) · H. Yu · W. Zeng · H.-Y. Liu
School of Chemistry and Chemical Engineering, Sun Yat-Sen University, Guangzhou 510275, People's Republic of China
e-mail: shaog@mail.sysu.edu.cn

Aldrich) was put in an alumina boat and a piece of aluminum foil ($50 \times 50 \times 0.3$ mm^3, 99.9%, Aldrich) was added above the SiO powder. The boat was placed at the central region of the horizontal alumina tube. The system was evacuated to a pressure of 10 Pa and the vacuum machine was turned off. The reactor was heated to 1300 °C at an increase rate of 10 °C min^{-1}, and maintained at 1300 °C for 4 h. After the reactor was cooled to room temperature at a rate of 20 °C min^{-1}, a thick layer of white, fluffy products were obtained on the surface of the foil [16–19].

The synthesized products were characterized by XRD (Shimadzu, equipped with Cu-K$_\alpha$ radiation, $\lambda = 0.15406$ nm), and the scanning rate of $0.02°s^{-1}$ was applied to record the pattern in the 2θ range of 10–100°. The morphology of the product was examined by SEM (Hitachi S-4800). The TEM and HRTEM images were investigated with a JEOL-2010 transmission electron microscopy, using an accelerating voltage of 200 kV.

Results and discussion

Figure 1 is the XRD pattern that may be indexed as a hexagonal structure of aluminum oxides. The intense peaks indicate that the prepared aluminum oxides have a high degree of crystallinity. The lattice constants calculated for the sample are $a = 0.4753 \pm 0.0010$ nm, $c = 1.300 \pm 0.006$ nm, which are quite in agreement with the reported values $a = 0.4758$ nm, $c = 1.299$ nm (α-Al$_2$O$_3$, JCPDS 10–0173).

The SEM image (Fig. 2) shows the alumina products with the morphology of ribbon. The nanoribbons grow on a large scale in an aligned manner with the length of ca. 100 μm. Their width changes greatly, and the thickness is
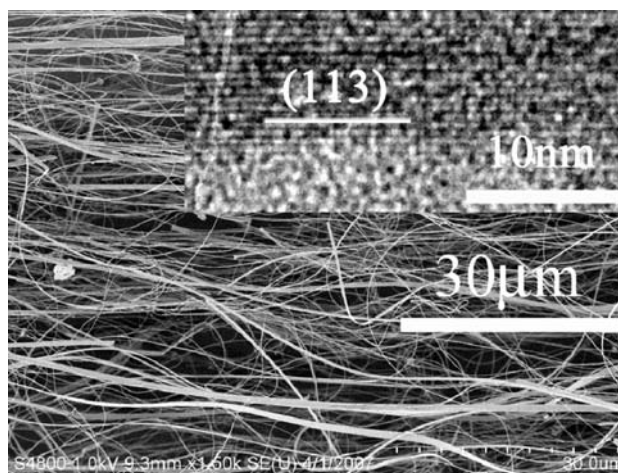
Fig. 2 SEM image of the typical α-alumina nanoribbons and HRTEM image (inset) showing (113) crystal plane
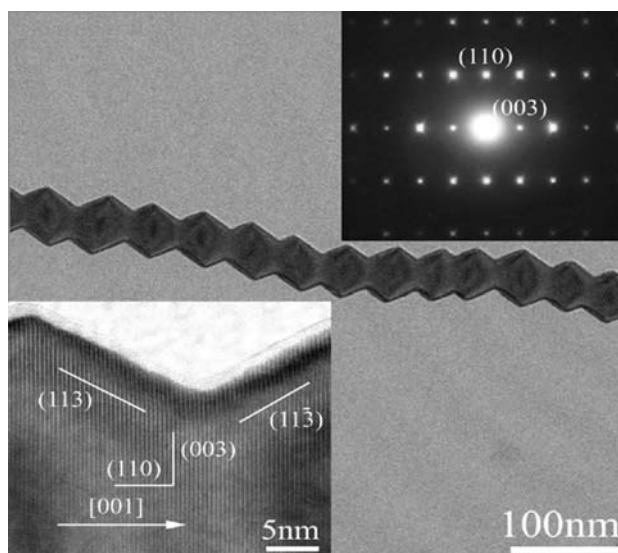
Fig. 3 TEM images of serrated α-alumina with reaction time of 0.5 h and selected area electron diffraction pattern (inset) and HRTEM image (inset)

ca. 60 nm judged from the image. The HRTEM image (Fig. 2, inset) exhibits the (113) crystal plane.

In an attempt to investigate the growth mechanism of alumina nanoribbons, the reaction time was reduced to 0.5 h and some other different new morphology was observed. Figure 3 shows a representative morphology of the products. They all have a saw-like morphology irrespective of the size, which can be called as nanosaws and their both sides are zigzag. The average width of the nanosaw is 50 nm and the length is larger than 1 μm.

The selected area electron diffraction of the nanosaw (Fig. 3, inset) shows bright diffraction spots, which reveals its single-crystal characteristics and high crystallinity. The diffraction spots can be indexed as the (110) and (003)

Fig. 1 XRD pattern of the α-alumina nanoribbons
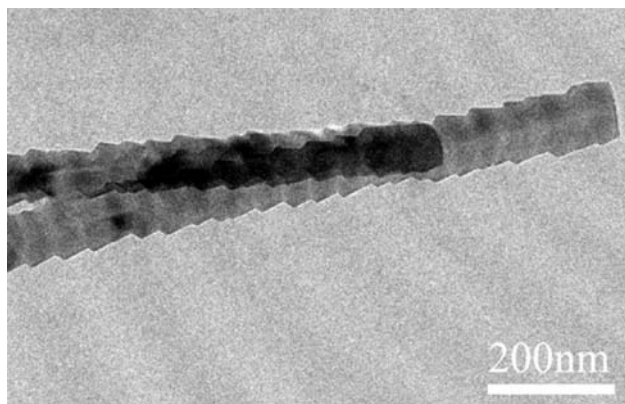
Fig. 4 TEM images of serrated α-alumina with reaction time of 1 h
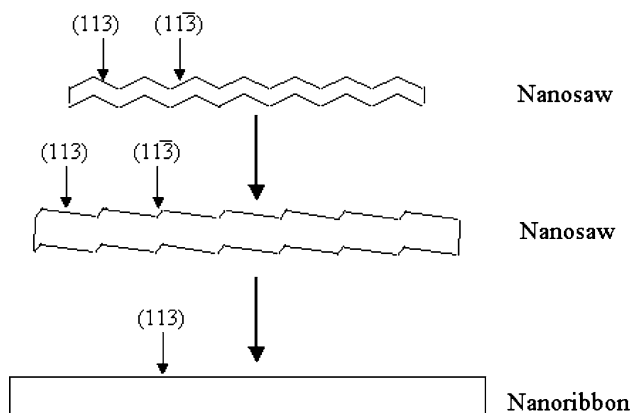
Fig. 5 A scheme of morphological evolution

planes of α-alumina. HRTEM technique was employed to investigate the zigzag nanostructure, which shows clear lattice pattern indicating its perfect single crystal structure (Fig. 3, inset). The crystalline planes may be indexed as (110) and (003) with the growth direction of [001]. The slope plane of the zigzag may be indexed as (113) and (11$\bar{3}$)planes with the intersection angle of 122.5°, which is in agreement with the calculated result (122.4°).

When the reaction time was changed to 1 h, the nanosaws of products became wider and smoother with the width of ca. 100 nm. Figure 4 shows the TEM image. Careful examination of the nanosaws' morphologies gives insight into the growth habits. As shown in Fig. 3, the nanosaw has sharp junction corners. The top/down surfaces of the building blocks could be indexed as ±(1–10) planes, and the side surfaces are enclosed by ±(113) and ±(11$\bar{3}$) planes, alternately. After further growth, ±(11$\bar{3}$) planes disappear and ±(113) planes remain (Fig. 3, inset), thus, the nanosaws become smoother on both sides (Fig. 4) and result in well-faceted nanoribbons. Figure 5 clearly demonstrates the scheme of morphological evolution from nanosaw to nanoribbon.

The chemical reaction involved in the experiment might be briefly described as [16]:

$$2SiO(g) \rightarrow SiO_2(g) + Si(g) \tag{1}$$

$$4Al(l) + 3SiO_2(g) \rightarrow 2Al_2O_3(s) + 3Si(s) \tag{2}$$

In the reactor, first solid SiO sublimated at high temperature to generate SiO vapor which then decomposed into Si and SiO_2 (Eq. 1), thus SiO produced SiO_2 as an oxidant. Afterwards, high temperature made Al liquefy and the molten Al reacted with SiO_2 to form alumina with high purity (Eq. 2). A passive oxidation reaction happened during the liquefaction process. A thin layer of alumina could protect the molten aluminum, which was responsible for the presence of liquid aluminum at 1300 °C under a pressure of 10 Pa. But Al(l) will slowly evaporate, and some production of aluminum fume can be at the same expected. Al(g) could react with SiO and give rise to alumina via another way described as follows [15]:

$$Al(g) + SiO(g) \rightarrow AlO_x(g) + Si(g), \quad x = 0.5, 1$$

$$AlO_x(g) + SiO(g) \rightarrow Al_2O_3(g) + Si(g)$$

$$Al_2O_3(g) \rightarrow Al_2O_3(s)$$
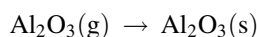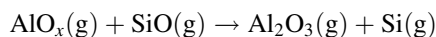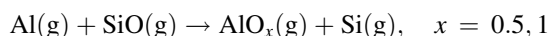
Conclusions

In summary, we have developed a new method for the synthesis of α-alumina nanoribbons. An interesting morphological evolution that nanoribbons resulted from the nanosaws was observed, which provided further details to understand the precise growth mechanism of nanoribbons.

References

1. Zhang C, Zhang X, Zhang X, Ou X, Zhang W, Jie J, Chang JC, Lee CS, Lee ST (2009) Adv Mater 21:1
2. Niu L, Shao M, Wang S, Lu L, Gao H, Wang J (2008) J Mater Sci 43:1510. doi:10.1007/s10853-007-2374-3
3. Huang MH, Mao S, Feick H, Yan H, Wu Y, Kind H, Weber E, Russo R, Yang PD (2001) Science 292:1897
4. Alivisatos AP (1996) Science 271:933
5. Zhao YS, Wu J, Huang J (2009) J Am Chem Soc 131:3158
6. Jung A, Natter H, Hempelmann R, Lach E (2009) J Mater Sci 44:2725. doi:10.1007/s10853-009-3330-1
7. Sawai O, Oshima Y (2008) J Mater Sci 43:2293. doi:10.1007/s10853-007-2031-x
8. Corrochano J, Cerecedo C, Valcarcel V, Lieblich M, Guitian F (2008) Mater Lett 62:103
9. Ye C, Zhang L, Fang X, Wang Y, Yan P, Zhao J (2004) Adv Mater 16:1019

10. Ma C, Ding Y, Moore D, Wang X, Wang ZL (2004) J Am Chem Soc 126:708
11. Hu JQ, Bando Y, Liu QL, Golberg D (2003) Adv Funct Mater 13:493
12. Hafiz J, Mukherjee R, Wang X, Cullinan M, Heberlein JVR, McMurry PH, Girshick SL (2006) J Nanopart Res 8:995
13. Shao MW, Shan YY, Wong NB, Lee ST (2005) Adv Funct Mater 15:1478
14. Shao MW, Zhang W, Wu ZC, Ni YB (2004) J Cryst Growth 265:318
15. Cerecedo C, Valcarcel V, Gomez M, Drubi I, Guitian F (2008) Adv Eng Mater 9:600
16. Valcarcel V, Souto A, Guitian F (1998) Adv Mater 10:138
17. Valcarcel V, Perez A, Cyrklaff M, Guitian F (1998) Adv Mater 10:1370
18. Valcarcel V, Cerecedo C, Guitian F (2003) J Am Ceram Soc 86:1683
19. Cerecedo C, Valcarcel V, Gomez M, Guitian F (2006) J Am Ceram Soc 89:323
20. Zhou J, Deng SZ, Chen J, She JC, Xu NS (2002) Chem Phys Lett 365:505
21. Xiao ZL, Han CY, Welp U, Wang HH, Kwok WK, Willing GA, Hiller JM, Cook RE, Miller DJ, Crabtree GW (2002) Nano Lett 2:1293
22. Wu WC, Wang XL, Wang DA, Chen M, Zhou F, Liu WM, Xue QJ (2009) Chem Commun 1043–1045
23. Yu C, Liu GH, Zuo BL, Tang YJ, Zhang T (2008) Anal Chim Acta 618:204
24. Lee HC, Kim HJ, Chung SH, Lee KH, Lee HC, Lee JS (2003) J Am Chem Soc 125:2882
25. Liu X, Wu ZG, Peng TY, Cai P, Lv HJ, Lian WL (2009) Mater Res Bull 44:160
26. Masuda H, Fukuda K (1995) Science 268:1466
27. Wakihara T, Hirasaki T, Shinoda M, Meguro T, Tatami J, Komeya K, Inagaki S, Kubota Y (2009) Cryst Growth Des 9:1260
28. Wang S, Shao MW, Lu L, Wang H, Gao HZ, Wang J (2008) Mater Chem Phys 112:230
29. Law M, Sirbuly DJ, Johnson JC, Goldberger J, Saykally RJ, Yang PD (2004) Science 305:1269